

壁面局部振动的管内射流流场模拟

王宏光, 朱志文, 葛利顺

(上海理工大学 能源与动力工程学院, 上海 200093)

摘要: 采用动网格技术和 $k-\varepsilon$ 两方程湍流模型, 通过求解二维非定常不可压雷诺时均 $N-S$ 方程, 对局部壁面振动的管内射流流场进行模拟, 分析局部壁面振动的振幅和频率对流动的影响。结果表明: 射流孔下游壁面静压随振幅、频率的增加而增加; 射流孔的平均流量随振幅的增加而减小, 随频率的增加而增加; 流量波动随振幅、频率的增加而增加, 高频率对流动的影响更加明显。研究结果为进一步研究振动表面小孔射流特征和振动叶片的气膜冷却问题提供参考。

关键词: 管内流动; 射流; 壁面振动; 非定常流动

中图分类号: TK124 文献标识码: A
DOI:10.16146/j.cnki.rndlgc.2015.01.010

引言

振动壁面会造成流体的扰动^[1-2], 进而影响流体与振动体表面的传热效果, 因此认识和掌握振动表面的流动规律, 对分析涡轮动叶片的热负荷与可靠性有重要意义。

但到目前为止, 对第一类传热面振动强化换热问题, 即涡轮动叶片振动与叶片冷却效果之间关系问题研究还没有见到相应的文献。

本研究将振动叶片气膜冷却孔附近流动问题, 简化为壁面局部振动的二维管内射流模型, 研究射流孔附近的壁面局部振动对流动状态的影响, 为进一步研究振动叶片的气膜冷却问题提供参考。

1 计算模型

计算模型如图1所示, 流动区域 ABCD 的长高比为 5:1, 振动区域 FG 位于 BD 的中心, 长度为 1; 射流孔位于 FG 的中心, 宽度为 0.1, 射流管长为 0.3。射流管随振动区域 FG 振动。

以水为工质, 进口边界 AB 采用速度入口, 给定进口流速 $v_0 = 20 \text{ m/s}$, 来流湍动能和湍动耗散率由经验公式计算得出^[3]。射流孔 E 给定总压 $P_0 = 199\ 640 \text{ Pa}$ 。下壁面 BFGD 和上壁面 AC 给无滑移

条件。出口边界 CD 给定静压 $P_1 = 101\ 325 \text{ Pa}$ 。

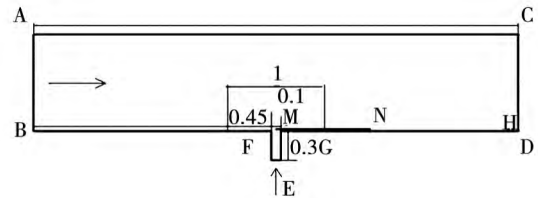


图1 简化模型图

Fig. 1 Simplified model diagram

采用 FLUENT 软件, 离散格式选择二阶迎风格式, 湍流模型选择 Realizable $k-\varepsilon$, 第一层网格距离边界 $0.000\ 2 \text{ m}$, 网格总数为 52 万, 时间步长取 $0.000\ 5 \text{ s}$, 隐式时间格式, 压力与速度的耦合采用 PISO 方法。图2为射流口附近的网格, 靠近壁面采用结构化网格, 其余位置采用非结构化网格。

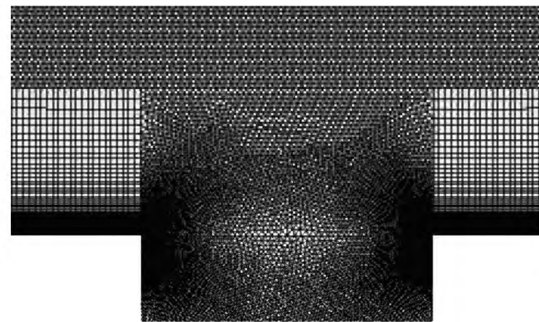


图2 射流出口静止时网格

Fig. 2 Grid when the outlet of the jet flow keeps still

2 计算结果

2.1 壁面不振动时射流流场计算

在壁面不振动的状态下, 计算管内流动。建立 xoy 坐标系, 坐标原点为 B 点, x 轴与 BD 重合且向右为正方向。在射流孔下游定义线段 MN, 距离壁

收稿日期: 2014-03-01; 修订日期: 2014-04-02

作者简介: 王宏光(1962-), 男, 辽宁开原人, 上海理工大学教授。

面为 $y=0.03\text{ m}$ x 坐标从 2.55 到 3.5 之间,通过该线段上的数据,分析壁面振动对流动的影响。经过网格无关性验证,证明网格密度满足要求。壁面不振动时线段 MN 上的静压分布如图 4 所示,图 9 是流场的速度云图。

2.2 壁面振动时射流流场计算

使壁面局部振动区域 FG 做简谐振动,振动从壁面与 x 轴重合时向 y 轴正方向开始,该时刻相位取为 0° 。振动与非振动区域的连接点 F 和 G 保持不动,保证了振动边与非振动边的连接。振动区域 FG 的位移和速度边界条件采用 UDF(自定义函数)控制^[4],下式给定其位移规律:

$$y = A \sin\left(\frac{2\pi}{T}t\right) \sin\left[\left(x - x_F\right) \frac{\pi}{L}\right]$$

式中: T —振动周期, μs ; L —点 F 与点 G 间的距离, m ; A —振幅, m ; x_F —F 点的 x 坐标。

振动的频率和振幅如表 1 所示,计算 6 个算例,比较振幅、频率和相位对流动的影响。

表 1 振动区域 FG 的振动边界条件

Tab.1 Boundary conditions for vibration in the vibration area FG

算例	I	II	III	IV	V	VI
频率 f/Hz	100	200	300	400	100	100
振幅 h/m	0.002	0.002	0.002	0.002	0.001	0.003

计算过程中检测出口边界上一点 H(5, 0.08) 的总压随时间变化情况,如图 3 所示。可以看出 3 个周期后,该点总压基本呈周期性变化,认为 3 个周期后的数据基本稳定。本研究选择第五周期的数据进行比较分析。

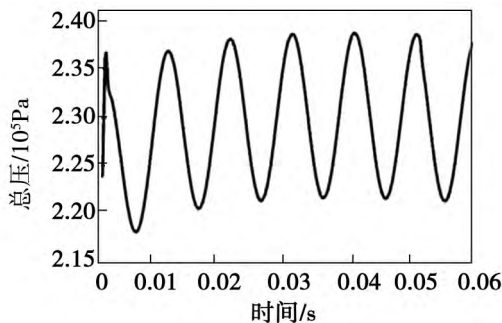


图 3 频率 100 Hz 时出口点 H 总压变化

Fig.3 Change in the total pressure at the point H of the outlet at a frequency of 100 Hz

2.2.1 频率对静压的影响

图 4 是在 FG 振幅为 0.002 m,相位角为 0° ,频

率为 100、200、300 和 400 Hz 时线段 MN 上静压分布对比图。可以看出随着频率的增加静压迅速增加。图 5 是线段 MN 上静压提取点的位置,研究斯特鲁哈尔数(St)与静压分布的关系。图 6 是 0° 相位时不同斯特鲁哈尔数 $St = \frac{fL}{U_\infty}$ 所对应线段 MN 上各点的静压分布,各点的静压随着 St 的增加而增加。

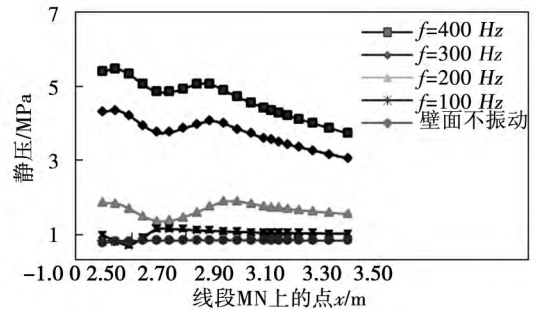


图 4 0° 相位角下线段 MN 不同频率的静压分布
Fig.4 Static pressure distribution in the line section MN at various frequencies at a phase angle of 0°

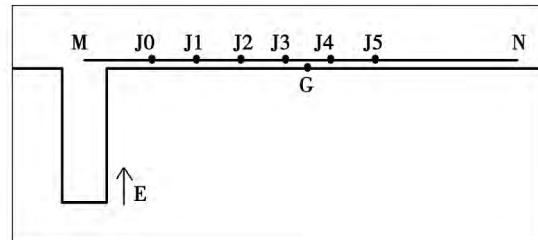


图 5 静压提取点在模型中的位置
Fig.5 Location of the point to obtain the static pressure in the model

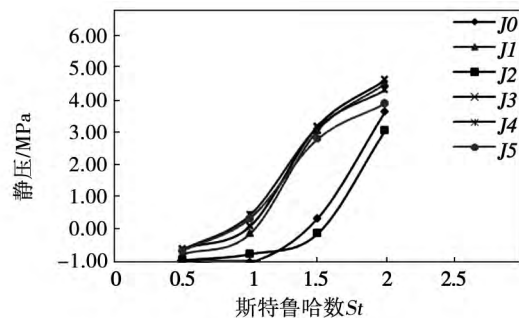


图 6 0° 相位角下各点随 St 的静压分布
Fig.6 Static pressure distribution at various points at a phase angle of 0° with St number

2.2.2 振幅对静压的影响

给定 FG 振动频率 100 Hz, 相位角 0° 振幅为 0.001、0.002 和 0.003 m 时线段 MN 上的静压分布如图 7 所示。可以看出振幅越高, 线段 MN 上静压波动幅度越大。从图可以看出由于振动频率相同, 不同振幅下静压分布的形态接近。

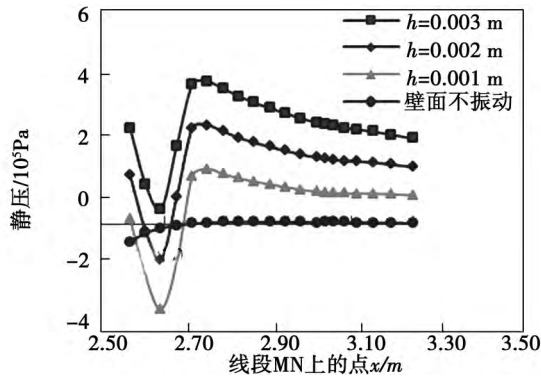


图 7 0° 相位角下线段 MN 不同振幅的静压分布
Fig. 7 Static pressure distribution in the line section MN at various amplitudes at a phase angle of 0°

2.2.3 相位对静压的影响

图 8 是 FG 振动频率 100 Hz, 振幅 0.002 m, 不同振动相位时, 线段 MN 上的静压分布图, 可以看出静压分布随壁面振动相位而变化。

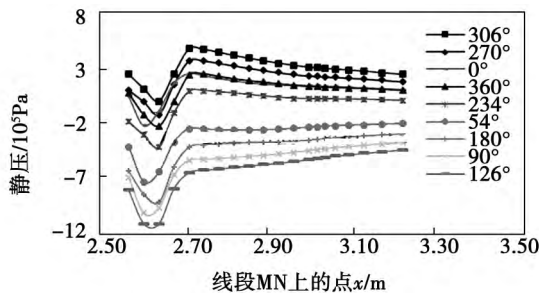


图 8 线段 MN 不同相位下的静压对比
Fig. 8 Contrast of the static pressures in the line section MN at various phases

2.2.4 速度云图对比

图 9 - 图 12 分别是壁面不振动时、算例 I、IV、VI 在相位角为 0° 时的速度云图对比。对比图 10 和图 11 可以看出不同振幅下的速度云图形态基本相同。对比图 10 和图 12 可以看出不同的频率下的速度云图有明显差别, 高频率振动对流动影响更加明显。

2.2.5 射流流量对比

各算例一个振动周期内的平均射流流量对比如表 2 所示。可以看出壁面振动时射流孔的平均射流流量大于不振动时的流量。振幅对射流流量 Q 影响如图 13 所示, 随振幅增加平均流量减小。频率对射流流量 Q 影响如图 14 所示, 随频率增加平均流量增大。

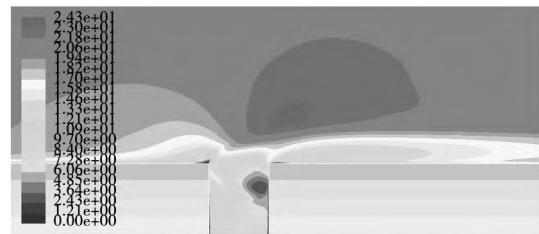


图 9 静态状态下的速度云图

Fig. 9 Atlas showing the velocity in a static state

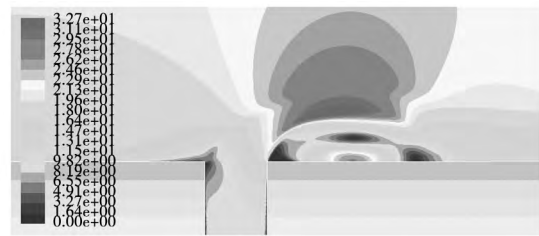


图 10 算例 I 下 0° 相位角的速度云图

Fig. 10 Atlas showing the velocity at a phase angle of 0° in the calculation case I



图 11 算例 VI 下 0° 相位角的速度云图

Fig. 11 Atlas showing the velocity at a phase angle of 0° in the calculation case VI

表 2 不同算例下通过射流口 E 的平均射流流量
Tab. 2 Average jet flow rate passing through the jet flow port E in various calculation cases

算例	不振动	I	II	III	IV	V	VI
平均流量 / kg·s ⁻¹	0.814 5	1.160 0	2.018 2	2.221 8	2.309 8	1.162 7	1.144 5

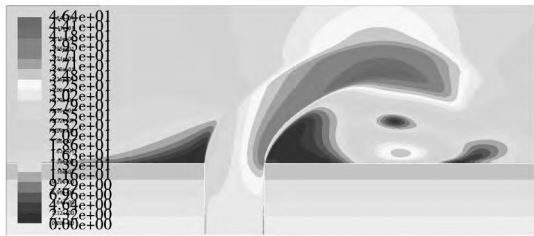


图 12 算例 IV 下 0° 相位角的速度云图
Fig. 12 Atlas showing the velocity at a phase angle of 0° in the calculation case IV

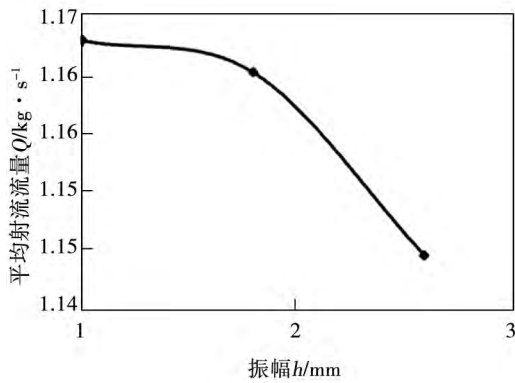


图 13 振幅对平均射流流量的影响
Fig. 13 Influence of the amplitude on the average jet flow rate

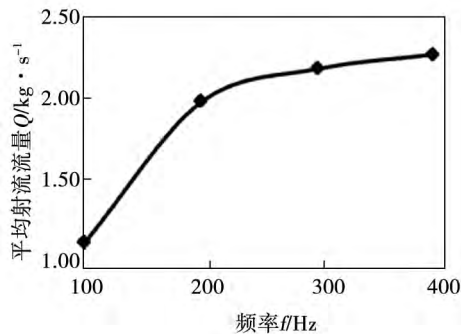


图 14 频率对平均射流流量的影响
Fig. 14 Influence of the frequency on the average jet flow rate

各算例射流流量随相位变化如图 15 所示。在 0° 与 90° 之间某些工况存在流量小于静态的情况。可以得出随振幅增加射流流量在一个周期内的波动增大。随频率增加射流流量的波动也增大。图 16 是算例 I 振动边界位移 Y 、射流流量 Q 和流场中

一点 $J(2.65, 0.03)$ 静压 P 在一个周期内的相位对比, 可见射流流量和流场静压都有较好的周期性。

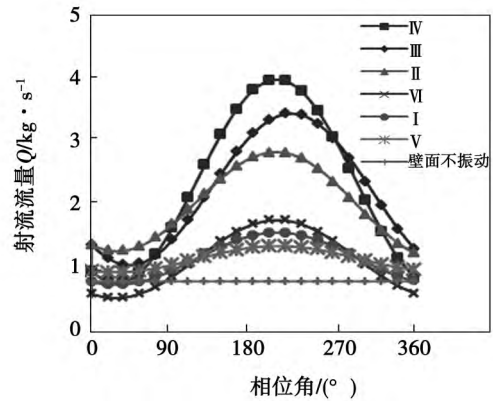


图 15 射流流量随相位角变化
Fig. 15 Changes of the jet flow rate with the phase angle

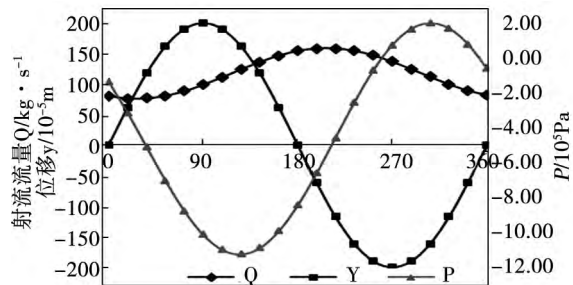


图 16 算例 I 综合对比
Fig. 16 Comprehensive contrast of the calculation case I with others

3 结论

根据以上的结果分析, 可以得到如下结论:

(1) 射流孔下游壁面附近的静压随振幅、频率和无量纲参数 St 的增加而增加, 静压分布随振动相位变化。

(2) 振动状态的射流孔平均射流流量高于静止状态。平均射流流量随振幅的增加而减小、随频率的增大而增大。射流流量的波动幅值随振幅和频率的增大而增大。

致谢

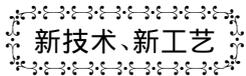
本研究得到教育部“高等学校博士学科点专项

科研基金联合资助课题(20123120110009)”资助, 特此致谢!

参考文献:

- [1] 裘进浩, 李大伟, 聂瑞等. 增加翼型升力的局部振动流动控制技术[J]. 南京航空航天大学学报, 2012, 44(5): 638-644.
QIU Jin-hao, LI Da-wei, NIE Rui, et al. Local vibration flow control technology for increasing the lift force of an aerofoil[J]. Journal of Nanjing University of Aeronautics & Astronautics, 2012, 44(5): 638-644.
- [2] 曹卫东, 张晓娣, 高一. 逆压梯度边界层壁面局部微振动诱导大涡结构[J]. 江苏大学学报, 2011, 32(5): 522-527.
CAO Wei-dong, ZHANG Xiao-di, GAO Yi. A large eddy configuration induced by local micro vibration on the wall surface of a boundary layer with a reverse pressure gradient[J]. Journal of Jiangsu University, 2011, 32(5): 522-527.
- [3] 王福军. 计算流体动力学分析-CFD 软件原理与应用[M]. 北京: 清华大学出版社, 2004.
WANG Fu-jun. CFD analysis-CFD software principle and applications[M]. Beijing: Tsinghua University Press, 2004.
- [4] 宿艳彩, 葛培琪, 闫柯等. 流体扰流不同方向振动圆柱换热特性数值分析[J]. 振动与冲击, 2011, 30(10): 221-223.
SU Yan-cai, GE Pei-qi, YAN Ke, et al. Numerical analysis of the heat exchange characteristics of a vibrating cylinder disturbed by a fluid in various directions[J]. Vibration and Shock, 2011, 30(10): 221-223.

(陈滨 编辑)



新技术、新工艺

核电站和热电站高压加热器的现代保护系统

DOI:10.16146/j.cnki.rndlgc.2015.01.011

据《Теплоэнергетика》2013 年 9 月刊报道, 中央锅炉涡轮机研究所的专家总结了高压加热器和防止水进入汽轮机的保护系统的运行经验。

分析了高压加热器管道破裂时蒸汽充满高压加热器空间所需时间, 并推导了所需时间的计算公式, 作出了基于该计算结果的高压加热器优化结构。

用实例证明了防止热电站和核电站汽轮机高压加热器壳体蒸汽空间水位升高的典型系统方案适用性。

分析了原有保护系统部件导致电站故障的缺陷。给出了无上述缺陷的现代保护系统的结构方案。

建立了主要保护部件(进口阀和止回阀)的数学模型并进行了计算研究。

提出了由中央锅炉涡轮机研究所制定的排除高压加热器保护系统假动作的平衡槽结构方案。

该高压加热器现代保护系统已被成功应用, 并在中国大亚湾核电站、伊朗布什尔核电站、俄罗斯加里宁核电站 4 号发电机组的汽轮机以及俄罗斯托夫斯克核电站的 2 号发电机组和保加利亚“科斯洛杜伊”核电站 5 号和 6 号发电机组的汽轮机上进行了试验。

(吉桂明 摘译)

cy of the thermal efficiency of the cycle and that of the second thermodynamic law will somewhat differ depending on the working medium chosen. With an increase of the temperature of the working medium at the outlet of the feedwater heater, the total irreversible loss and net output power of the cycle will keep declining while the thermal efficiency of the cycle and that of the second thermodynamic law will first increase and then decrease. Under the same operating condition, the thermal efficiency of the recuperative organic Rankine cycle and that of the second thermodynamic law will be higher than that of the organic Rankine cycle, however, those results of the net output power and total irreversible loss of the cycle will be to this contrary. **Key Words:** organic dry fluid, recuperative organic Rankine cycle, performance analysis

不同状态方程计算螺杆膨胀机膨胀过程的比较 = Comparison of the Expansion Process of a Screw Expander as Calculated by Using Various State Equations [刊, 汉] YING Zhen-gen, MA Xiao-li (School of Mechanical Engineering, Quzhou College, Quzhou, China, Post Code: 324000), TANG Chang-liang (Engineering Thermophysics Research Institute, Chinese Academy of Sciences, Beijing, China, Post Code: 100190) // Journal of Engineering for Thermal Energy & Power. -2015, 30(1). -31-36

The expansion process of a screw expander is the basic one in its operation and to employ the actual gas state equation to calculate this process can facilitate to analyze any problem. A general method for calculating the expansion process was given and the formula for calculating the expansion process were derived by using RKS equation and BB equation respectively and for the expansion process of the organic working medium R245fa in the screw expander, the RKS equation and BB equation were compared with the working medium physical property calculation software RefProp and a calculation was also performed. It has been found that both RKS and BB equation have a relatively high calculation precision, however, the RKS equation has an even higher calculation precision and more suitable for calculating the expansion process of a screw expander with R245fa serving as the working medium. **Key Words:** screw expander, expansion process, RKS equation, BB equation

壁面局部振动的管内射流流场模拟 = Numerical Simulation of the Jet Flow Field Inside a Tube With Its Wall Surface Being Locally Vibrated [刊, 汉] WANG Hong-guang, ZHU Zhi-wen, GE Li-shun (College of Energy Source and Power Engineering, Shanghai University of Science and Technology, Shanghai, China, Post Code: 200093) // Journal of Engineering for Thermal Energy & Power. -2015, 30(1). -37-41

By using the motive grid technology and equation-based two turbulent flow models and through seeking solutions to

the two-dimensional unsteady incompressible Reynolds time-averaged N-S equation ,the authors conducted a numerical simulation of the jet flow field inside a tube with its wall surface being locally vibrated and analyzed the influence of the amplitude and frequency of the local wall surface vibration on the flow. It has been found that the static pressure on the wall surface at the downstream of the jet flow holes will increase with an increase of the amplitude and frequency. The average flow rate of the jet flow holes will decrease with an increase of the amplitude and increase with an increase of the frequency. The fluctuation in the flow rate will increase with an increase of the amplitude and frequency. The high frequencies affect the flow more conspicuously. The research findings can offer reference for further study of the jet flow characteristics of small holes on the wall surface being vibrated and the air film cooling of blades being vibrated. **Key Words:** flow inside a tube ,jet flow ,vibration on wall surfaces ,unsteady flow

饱和多孔介质自然对流数学模型与实验研究 = **Mathematical Model for Natural Convection in a Saturated Porous Medium and Its Experimental Study** [刊 汉] YANG Wei ,XUE Si-han ,LIU Qin-jian (College of Architectural Engineering ,Liaoning University of Engineering Technology ,Fuxin ,China ,Post Code: 123000) ,ZHANG Shu-guang (College of Civil and Traffic Engineering ,Liaoning University of Engineering Technology ,Fuxin ,China , Post Code: 123000) //Journal of Engineering for Thermal Energy & Power. -2015 ,30(1) . -42 -47

With the fluid flow and heat transfer between a fluid and a solid serving as the object of study and changes of the density of the fluid with the temperature being taken into account ,the local heat balance was corrected by introducing the Brinkman-Forchheimer extended Darcy model ,a numerical model for natural convection of saturated porous media randomly deposited was set up and a calculation was performed by using finite volumetric method. By making use of a self-developed cubic porous medium test rig having a constant temperature difference at both sides ,the authors conducted an experimental verification of the numerical model in question. The comprehensive numerical calculation and test results show that the maximum flow speed inside the square cavity of the porous medium will increase with an increase of the temperature difference and Ra number and appear at a location nearing both high temperature wall surface and low temperature one. With an increase of the Ra number ,the isolines of the temperature will change from being almost parallel to the high and low temperature wall surface to being closely perpendicular to them. Nu number on the high temperature wall surface will assume a linear ascending tendency and the \overline{Nu} on the high temperature wall surface will increase with an increase of Ra . When $Ra < 102$, \overline{Nu} will maintain within 12. When $102 < Ra < 10^6$, \overline{Nu} will rapidly increase from 11. 4 to 276. 4. When $Ra > 106$, \overline{Nu} will increase at a very small speed. **Key Words:** saturated porous medium ,convection-based heat exchange ,mathematical model ,experimental study